

SOME PROBLEMS INVOLVED IN THE NUMERICAL SOLUTIONS OF TIDAL HYDRAULICS EQUATIONS

D. LEE HARRIS and CHESTER P. JELESNIANSKI

U.S. Weather Bureau, Washington, D.C.

ABSTRACT

The linearized two-dimensional hydrodynamic equations are presented in a manner which displays the principal assumptions involved. Several approximations are developed for the partial derivatives, and boundary conditions in finite difference form and the associated errors are discussed. The procedure for establishing a finite difference analog of the equations of motion and boundary conditions is illustrated, and computational stability for the solution of some simple problems is illustrated by means of examples.

The physical and computational problems associated with the introduction of friction in the computational model are discussed. It is concluded that friction should be neglected in many problems but that it must be considered in others.

1. INTRODUCTION

Tidal hydraulics is concerned with flow and the effects of flow in shallow basins in which the flow is generally dominated by long-period gravity waves, such as the tides, generated in an adjacent sea or ocean. Interest is generally centered in the vertical motion of the free surface and the horizontal currents. Sometimes it is necessary to recognize a two-layered structure resulting from salt water intrusion or a thermocline. Sometimes it is sufficient to consider only one space dimension. The horizontal boundaries of the basin may be very irregular and may vary with time, but their existence is an essential part of the problem. Energy may enter the basin through the open portion of the boundary in the form of wave motion, or through the free surface as wind stress. Energy is presumed to be dissipated through bottom friction.

The equations which govern all tidal hydraulic flows are too complex to permit a ready solution in any but the most simple problem. Therefore, most investigations are conducted with the aid of models in which one attempts to include only those phenomena which he believes to be most significant to the investigation. These models may be analogous, such as the familiar hydraulic models and the mechanical tide-predicting machine; they may require the digital or analytic solution of a set of differential equations, or the statistical analysis of observations. For maximum effectiveness, all models, physical and statistical as well as dynamic, should be based on a mathematical analysis of the physical problem. However, useful results can be obtained from both hydraulic and statistical models, even though this process is not fully developed.

The application of digital calculation on an electronic computer to the statistical analysis of storm surge generation has been discussed by Harris [7], Harris and Angelo

[9], and Pore [19]. A similar application of digital calculations to the analysis and prediction of tides is given by Harris, Pore, and Cummings [10].

This paper is concerned primarily with the application of digital calculations to the solution of the hydrodynamic equations in two horizontal dimensions. The mathematical background will be discussed from the point of view of showing both the weaknesses and strengths of digital calculations as compared to other methods of solving similar problems. No attempt is made at a rigorous development of the ideas presented if these can be found in a reasonably available reference. Examples of the calculations made by several of the computational models for very simple basins are presented.

2. THE HYDRODYNAMIC EQUATIONS

Since interest is centered in the horizontal flow and the motion of the free surface, it is natural that the principal simplification should take the form of a vertical integration of the primitive equations. This process can be carried out with various degrees of rigor. Many writers have derived the equations of motion and continuity directly in integrated form, but this procedure does not show the approximations involved nearly so clearly as the derivation based on the integration of the primitive equations. The techniques of this integration have been shown by Haurwitz [11], Welander [24], Fortak [4], and Platzman [18]. Nearly all of the other derivations can be obtained as special cases of that given by Fortak.

The two-dimensional hydrodynamic equations may be stated in either of two equivalent forms. Until the introduction of digital computations with these equations, the form based on the mean current velocities was generally preferred. Since then the use of the volume transport

vector has gained popularity. The reason for this will be given in a later section. A form of the volume transport equations which contains most of the terms used by any worker in this field and a few error terms that must be discarded to obtain a solution are given below. This form would be valid if (1) the fluid were homogeneous; (2) the pressure were given by the hydrostatic equation; and (3) there were no surface waves. (Surface waves, not recognized in this model, will produce significant effects on sea level in some regions (Harris [8]).)

$$\begin{aligned} \frac{\partial U}{\partial t} + gD \left(1 + \frac{h}{D}\right) \frac{\partial h}{\partial x} + \frac{D}{\rho} \left(1 + \frac{h}{D}\right) \frac{\partial p_a}{\partial x} \\ - \frac{1}{\rho} [(^{(x)}\tau_h - (^{(x)}\tau_{-D})] - fV = \frac{\partial}{\partial x} \left(\frac{U^2}{D+h} \right) \\ + \frac{\partial}{\partial y} \left(\frac{UV}{D+h} \right) + \frac{\partial}{\partial x} \int_{-D}^h (u')^2 dz \\ + \frac{\partial}{\partial y} \int_{-D}^h (u'v') dz, \quad (1) \end{aligned}$$

$$\begin{aligned} \frac{\partial V}{\partial t} + gD \left(1 + \frac{h}{D}\right) \frac{\partial h}{\partial y} + \frac{D}{\rho} \left(1 + \frac{h}{D}\right) \frac{\partial p_a}{\partial y} \\ - \frac{1}{\rho} [(^{(y)}\tau_h - (^{(y)}\tau_{-D})] + fU = \frac{\partial}{\partial x} \left(\frac{UV}{D+h} \right) + \frac{\partial}{\partial y} \left(\frac{V^2}{D+h} \right) \\ + \frac{\partial}{\partial x} \int_{-D}^h (u'v') dz + \frac{\partial}{\partial y} \int_{-D}^h (v')^2 dz, \quad (2) \end{aligned}$$

$$\frac{\partial h}{\partial t} + \frac{\partial U}{\partial x} + \frac{\partial V}{\partial y} = 0; \quad U = \int_{-D}^h u dz, \quad V = \int_{-D}^h v dz \quad (3)$$

u, v , components of horizontal motion

$u' = u - U/(D+h)$

$v' = v - V/(D+h)$

ρ = density of water

p_a = atmospheric pressure

$(^{(x)}\tau_h, (^{(y)}\tau_h)$, components of surface stress; $(^{(x)}\tau_{-D}, (^{(y)}\tau_{-D})$, components of bottom stress

D = depth of undisturbed fluid

h = disturbance in the height of free surface

g = acceleration of gravity

f = Coriolis parameter

Since the atmospheric pressure and the surface stresses are not significantly affected by the water motions being considered in this paper, it must be assumed that they will be supplied from other sources. Consideration of the frictional dissipation terms will be deferred to the end of the paper, partly from lack of knowledge of the proper friction law, and partly to avoid certain complications that may arise in the discussion of computational stability if friction is introduced too early. The integrals in equations (1) and (2) are also neglected for lack of information required to compute them.

The boundary condition natural to the problem is no flow across a closed boundary.

The principal features of tidal hydraulics computations can be better displayed in a linearized version of equations (1)–(3). We may return to the initial set of equations for correction terms as needed or to determine the nature of the errors resulting from neglected terms. The linearized equations may be given in the form:

$$\frac{\partial U}{\partial t} + gD \frac{\partial h}{\partial x} - fV + KU/D = -D\rho^{-1} \frac{\partial p_a}{\partial x} + (^{(x)}\tau_h/\rho) \quad (4)$$

$$\frac{\partial V}{\partial t} + gD \frac{\partial h}{\partial y} + fU + KV/D = -D\rho^{-1} \frac{\partial p_a}{\partial y} + (^{(y)}\tau_h/\rho) \quad (5)$$

$$\frac{\partial h}{\partial t} + \frac{\partial U}{\partial x} + \frac{\partial V}{\partial y} = 0 \quad (6)$$

$$KU/D = \frac{(^{(x)}\tau_{-D}}{\rho}; \quad KV/D = \frac{(^{(y)}\tau_{-D}}{\rho}$$

3. FINITE DIFFERENCE EQUATIONS

To obtain a digital solution of the above equations it is necessary to approximate the differential quotients by finite differences at discrete points in time and space. Suitable approximations can be derived from Taylor Series expansions of the functions as illustrated below:

$F(x+\Delta x)$ may be written as

$$\begin{aligned} F(x+\Delta x) = F(x) + \frac{dF(x)}{dx} \Delta x + \frac{d^2F(x)}{dx^2} (\Delta x)^2/2! \\ + \frac{d^3F(x)}{dx^3} (\Delta x)^3/3! + \dots \quad (7) \end{aligned}$$

If only the first two terms of this series are considered, one obtains

$$\frac{dF(x)}{dx} = \frac{F(x+\Delta x) - F(x)}{\Delta x} + \epsilon_1 \quad (8)$$

where the error, ϵ_1 , is given by

$$\epsilon_1 = \frac{d^2F(x)}{dx^2} \frac{\Delta x}{2} \quad (9)$$

Equation (8) is called a two-point forward difference. A better approximation for many purposes can be obtained by considering a second Taylor expansion, $F(x-\Delta x)$ which may be written as

$$\begin{aligned} F(x-\Delta x) = F(x) - \frac{dF(x)}{dx} \Delta x + \frac{d^2F(x)}{dx^2} (\Delta x)^2/2! \\ - \frac{d^3F(x)}{dx^3} (\Delta x)^3/3! + \dots \quad (10) \end{aligned}$$

Subtraction of (10) from (7) gives

$$\frac{dF(x)}{dx} = \frac{F(x+\Delta x) - F(x-\Delta x)}{2\Delta x} + \epsilon_2 \quad (11)$$

where the error, ϵ_2 , is given by

$$\epsilon_2 = \frac{d^3 F(x)}{dx^3} \frac{(\Delta x)^2}{3!} \quad (12)$$

Equation (11) is called a central difference form. Other approximations to the differential quotients can be constructed as needed by extensions of this principle. A three-point forward difference that will be needed later is

$$\frac{dF}{dx} = \frac{1}{2\Delta x} [-3F(x) + 4F(x + \Delta x) - F(x + 2\Delta x) + \epsilon_3];$$

$$\epsilon_3 = 4 \frac{d^3 F(x)}{dx^3} \frac{(\Delta x)^2}{3!} \quad (13)$$

The dependence of F on both x and y can be considered by means of a Taylor expansion of the function in two dimensions. One such expansion which will be needed later is given by

$$\frac{\partial F(x, y)}{\partial x} = \frac{1}{(4a+2b)\Delta s} [a\{F(x+\Delta x, y+\Delta y) - F(x-\Delta x, y+\Delta x) + F(x+\Delta x, y-\Delta y) - F(x-\Delta x, y-\Delta y)\} + b\{F(x+\Delta x, y) - F(x-\Delta x, y)\}] \quad (14)$$

$$\Delta x = \Delta y = \Delta s$$

Equation (14) can be written in a more compact form as

$$\frac{\partial F(x, y)}{\partial x} = \frac{1}{(4a+2b)\Delta s} \begin{vmatrix} -a & 0 & a \\ -b & 0 & b \\ -a & 0 & a \end{vmatrix} F(x, y) \quad (15)$$

This form has been derived in a somewhat different manner by Shuman [23] who sets $a=1$, $b=2$, and calls this a "filter factor form". The reason for this name will be given later. It should be noted that if $a=0$ and $b=1$, equation (15) reduces to (11). Lauwerier [13] used a form of (15) in which $a=1$, $b=0$, and showed that this has several desirable properties not possessed by (11).

Equation (11) is the most widely used approximation for $\partial F/\partial x$ in the digital solution of problems whose solutions are expected to be some type of wave. It is frequently unacceptable for the time derivative in dealing with diffusion problems; however, tidal hydraulics is mainly concerned with waves, and it appears that satisfactory solutions for many problems can be based on equation (11). By combining equation (11) with equations (4)–(6) and ignoring the bottom stress, the following equations are obtained.

$$U_{i,j}^{m+1} = U_{i,j}^{m-1} - gD_{i,j} \frac{\Delta t}{\Delta s} [h_{i+1,j}^m - h_{i-1,j}^m] + 2\Delta t [fV_{i,j}^m + {}^{(x)}\tau_{i,j}^m] \quad (16)$$

$$V_{i,j}^{m+1} = V_{i,j}^{m-1} - gD_{i,j} \frac{\Delta t}{\Delta s} [h_{i,j-1}^m - h_{i,j+1}^m] - 2\Delta t [fU_{i,j}^m - {}^{(y)}\tau_{i,j}^m], \quad (17)$$

$$h_{i,j}^{m+1} = h_{i,j}^{m-1} - \frac{\Delta t}{\Delta s} [U_{i+1,j}^m - U_{i-1,j}^m + V_{i,j+1}^m - V_{i,j-1}^m] \quad (18)$$

Here the notation $F_{i,j}^m$ means $F(i\Delta x, j\Delta y, m\Delta t)$. The pressure gradient term has been combined with the surface stress term to obtain a simpler equation because both of these terms must be supplied and the pressure term is not the source of any computational difficulties. The density has been absorbed into the symbol τ in order to simplify the notation in the remainder of the paper. This does not call for any numerical changes as the constant density may be taken as one unit, but in dimensional checks it must be remembered that τ is stress per unit mass.

An examination of equations (16)–(18) shows that the calculations of U and V for even time steps can be effected by using h values for only odd time steps and vice versa. Calculation of U and V at points i, j , in this manner does not require a knowledge of h at the same points. Likewise the calculation of h at i, j does not require any knowledge of U or V at i, j . In short, this computational grid consists of several interlocking sub-grids such that the calculation of h on one grid requires a knowledge of U, V one time step removed on a different grid. This feature has been discussed extensively by Platzman [17], [18], and Welander [24]. Many workers take advantage of this fact to reduce the machine time required for a computation. Others prefer to compute on all available interlocking grids, and to compare the semi-independent solutions to obtain a measure of the error involved in the calculations. In this study, the field values are computed on each and every grid point including the boundaries for every time interval. The calculations are staggered neither in time nor space.

4. COMPUTATIONAL STABILITY

Any finite difference expression for differential quotients generally involves both round-off and truncation errors, since the calculations can be carried out only to a finite number of decimal places, and because the approximation for the derivative is based on an incomplete description of the functions. It can be shown that the time dependence of the error is approximated by functions of the type

$$\epsilon = A(x, y) e^{\alpha + i\beta} t \quad (19)$$

If A and α are both different from zero, the error will grow with time until it ultimately exceeds the true solution, and the computation is said to be unstable. No method has been found for insuring that $A(x, y) = 0$. Theorems have been developed for insuring that α will vanish in certain cases. These theorems generally impose a limiting value for Δt in the form

$$\Delta t \leq M \quad (20)$$

where M is a linear function of Δs and may depend on

other parameters of the problem. The form of equation (20) depends on the particular finite difference prediction equations employed, and may be altered if any term is changed, or if any new terms are added.

It is rarely possible to establish the requirements for computational stability for geophysical hydrodynamic problems in any rigorous manner. Theory can be used as a guide in the construction of finite difference systems which may be sufficiently stable for practical problems but the final proof of stability must come from test calculations. One of the principal symptoms of computational instability is a growth or decay of energy in the system, which does not result from those terms of the equations which should add or subtract energy. Thus an effective test for instability can be constructed by introducing a disturbance into the numerical model and monitoring the total energy of the solution through several oscillations of the primary mode when both forcing terms and dissipating terms are omitted from the equations.

Since computational instability usually takes the form of an unreasonable growth of energy in the system, it was initially thought that the instability found in the solution of practical problems resulted from using too low a value for the frictional dissipation, and efforts were made to control this instability by the introduction of larger friction coefficients for the additional dissipation terms.

One of the first thorough examinations of the computational stability of a tidal hydraulics problem was published by Fischer [3]. He used forward time differences for the transport terms U and V , and backward time differences for the height. Central differences were used for all space derivatives. His stability analysis indicated that

$$\Delta t \leq K/Df^2, \quad f \neq 0, \quad \text{and} \quad \Delta t \leq \Delta x/\sqrt{gD/2} \quad (21)$$

with the notation used in this paper. See Appendix 5.

Thus very short time intervals have to be used with this system if the water is very deep, and calculations near the equator would be impossible.

The form of equations (9) and (12) shows that the truncation error is highest in the higher-order harmonics of the basin. A little reflection will show that this is also true of the round-off error. Thus one may expect to reduce instability by introducing some process which will remove all traces of the highest harmonic and will damp the other high harmonics. This process is called "filtering" or "smoothing." It is especially important and especially difficult to treat properly when non-linear terms of the equations are being considered because of the tendency of non-linear terms to divert energy from the principal harmonics to those with both higher and lower wave numbers. Unfortunately, most filters which remove the unwanted higher harmonics of the system also change the energy content of other harmonics as well, and great care must be required in constructing filters which remove the difficult-to-treat high harmonics without

seriously affecting the phenomena being studied. Extensive discussions of the construction of numerical filtering functions have been given by Shuman [22] and Holloway [12].

It can be shown by methods discussed by Shuman and Holloway, that the numerical filter,

$$\tilde{F}(x) = \frac{1}{4} [F(x-\Delta x) + 2F(x) + F(x+\Delta x)]$$

will eliminate the harmonic with a wavelength of $2\Delta x$, which is found to be the most troublesome, without introducing a phase shift or changing the mean value of $F(x)$ over any extended range. Extending the above filter to two dimensions as in Appendix 4 justifies setting $a=1$, $b=2$ in equation (15) and calling the resulting central difference form the "filter factor form." With these values of a and b , the filter factor form eliminates wavelengths of $2\Delta x$ in either the x or y directions. Several other types of smoothing can be used to improve the computational stability. The selection of the best method for a particular problem requires an understanding of the physical processes which are important to the problem. Some subjective judgment based in part on the solution of identical problems with two or more different values of Δx and Δt , is nearly always necessary.

5. FACTORS FAVORING THE TRANSPORT FORM OF THE INTEGRATED EQUATIONS

Continuity considerations require that the total transport through a channel of variable cross section must be a reasonably smooth function of distance. Thus the mean speed increases in restricted passages and decreases in more open regions. Since the mean speed varies more with position than the total transport, the higher harmonics in a Fourier expansion of the speed have larger amplitudes than the corresponding harmonics in a Fourier expansion of the total transport field. The increased importance of the higher harmonics causes greater distortion of the true solution by smoothing or filtering operators when mean velocity terms are used instead of the transport terms. Neither of these deficiencies in the mean velocity equations exists when analytic solutions of the equations are obtained. Thus they result only from the application of finite difference methods.

6. FINITE DIFFERENCE REPRESENTATION OF THE BOUNDARY CONDITIONS

Much of the present understanding of the computational stability and the use of smoothing functions in tidal hydraulics problems stems from the extensive studies of numerical weather prediction. The basic equations of numerical weather prediction and tidal hydraulics are very similar; the principal differences are the greater importance of the non-linear terms in the meteorological

problem and the greater importance of variable coefficients in the tidal hydraulics problem.*

However, the situation with respect to boundary conditions is vastly different. There are no natural boundaries in most meteorological problems. Consequently, the meteorologist chooses artificial boundaries in regions distant from that of major interest so that the probability of boundary error penetration into the region of major interest is at a minimum. However, the meteorologist has the advantage of many observations at many levels throughout his region of interest every day. These observations provide realistic initial values at frequent intervals and partially offset the necessity of working with rather poorly stated boundary conditions.

In tidal hydraulics and oceanography, on the other hand, the boundaries are often well defined. Most of the information which can be used in evaluating models comes from the boundary, and observations from the interior of the fluid which could be used to provide initial conditions

* Useful first approximations to the solution of many meteorological problems can be obtained with models which eliminate gravity waves, but retain the effects of the earth's rotation. The gravity waves are essential to the tidal hydraulics problem, but a first approximation may often be obtained without consideration of the rotation of the earth. There are some problems in both fields in which the conditions are the reverse of those stated above, and many problems in both fields in which both gravity and rotation are important. Thus this is not considered to be a fundamental difference between the two fields.

are very rare. Consequently the need for accurate statements of the boundary conditions is much greater than in meteorology. The simplest statement of the boundary conditions is obtained for a closed rectangular region of dimensions L W ; in this case the boundary conditions become

$$u(0)=u(L)=0$$

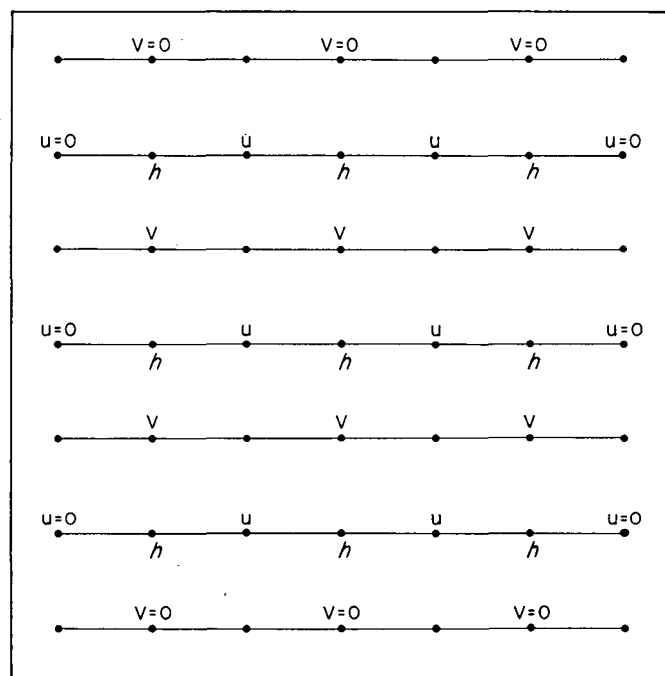
$$v(0)=v(W)=0$$

A solution which is consistent with the true boundary conditions and the central difference formulation of the problem can be obtained from the calculation illustrated in figure 1a. Values supplied or computed for odd time intervals are shown above the computation point; values computed for even time intervals are shown below the line. If the Coriolis term must be included, a somewhat less satisfactory procedure results, illustrated in the same manner in figure 1b. Here the boundary must be thought of as moving a distance of Δs between time steps and the entire procedure must be considered as a gross approximation. Real basins rarely have straight line boundaries, but if Δs is small relative to the basin, the true boundary can be approximated by a short section of a zigzag boundary constructed on the above principle. Calcula-

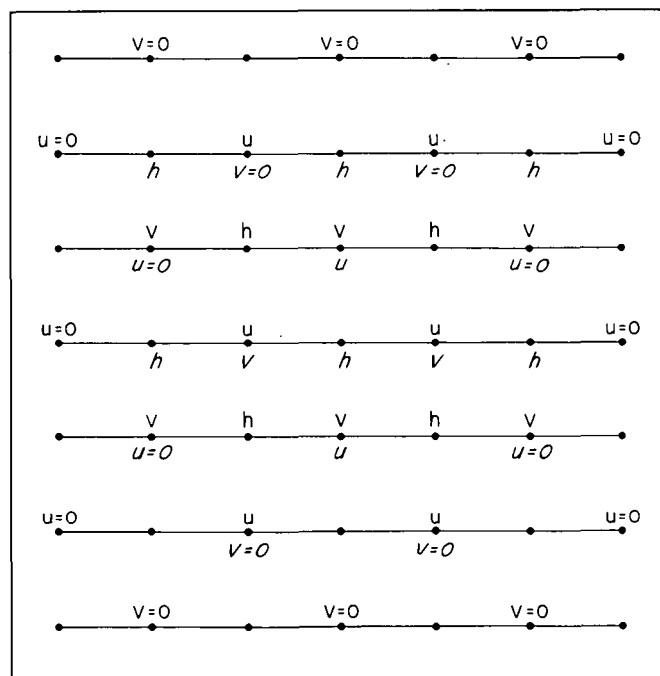
Boundary conditions

$u=0$ at $x=0$, and $x=L$

$v=0$ at $y=0$, and $y=W$



a



b

Vertical letters (u) are odd times
Slant letters (v) are even times

FIGURE 1.—Schematic illustration of a simple representation of the computation scheme and boundary condition in the digital solution of the hydrodynamic equations for a rectangular basin: (a) without rotation, (b) with rotation.

tions made with this type of boundary show that the main features of the flow can be reproduced with reasonable accuracy (Hansen [5], [6]; Welander [24]). Nevertheless, the many fictitious corner points introduced by this zigzag boundary are source points for small-scale disturbances not germane to the problem, and the details of the solution obtained with this system are of questionable value. The system does not provide values of h at the coast where they are most needed and where most of the verification data are to be found.

An alternate system of approximating the true boundary without the use of false corner points has been developed by Platzman [18]. He requires that the flow be parallel to the generalized coast at the coastline, and applies the continuity equation for a calculation of the mean height in each computation square of length Δs which is crossed by the coastline.

A form of the boundary conditions which gives h at the coast and which we believe to be new is given below. This form presupposes that transport and height terms are calculated at each point of the grid system. If there is no transport across the line $x=0$, equation (4) reduces to the form

$$gD \frac{\partial h}{\partial x} = fV + {}^{(x)}\tau \quad (24)$$

If D is constant, combining equations (24) and (13) gives

$$h_{0,j}^m = \frac{1}{3} \left[4h_{1,j}^m - h_{2,j}^m - \frac{2\Delta s}{gD_{0,j}} \{fV_{0,j}^m + {}^{(x)}\tau_{0,j}^m\} \right] \quad (25)$$

If D vanishes at the coast, equation (24) for $\partial h/\partial x$ is indeterminate. This possibility can be avoided by introducing the identity

$$D \partial h / \partial x = \partial(Dh) / \partial x - h \partial D / \partial x \quad (26)$$

When this expression is combined with (24) and (13) one obtains

$$h_{0,j} = \frac{4h_{1,j}^m D_{1,j} - h_{2,j}^m D_{2,j} - \frac{2\Delta s}{g} \{fV_{0,j}^m + {}^{(x)}\tau_{0,j}^m\}}{4D_{1,j} - D_{2,j}} \quad (27)$$

The term, $D_{0,j}$ does not appear in this expression, so the solution does not become indeterminate when $D_{0,j}$ vanishes at the shore. However, it reduces to (25) when D is constant. The acceptability of this expression when $D_{0,j}=0$ at the coast has not been tested but it will be shown below that this form does lead to an improvement in the calculations for some cases of variable but non-vanishing depths at the shore. Expressions for the boundary conditions on the other boundaries can be developed in a similar manner.

It is very convenient when obtaining quantitative analytic solutions and when discussing most of the problems associated with numerical solutions to consider only rectangular regions. However, this also presents problems

concerning the proper expressions for the variables at the corner points which are common to both boundaries. The ideal solution should deal with actual, e.g., curvilinear boundaries, and the problem of corner points should ultimately vanish. Hence this is not considered a fundamental problem; however at the present stage of development it is essential that corner points be considered in a manner which will minimize errors. Methods for doing this are presented in Appendix 3.

7. POTENTIAL ADVANTAGES OF DIGITAL SOLUTIONS

In spite of the difficulties cited above, the digital method of solving the tidal hydraulics problem offers certain advantages that cannot be obtained by other means. The most obvious advantage is that the finite difference formulation of the problem permits a much better approximation to the actual wind stress and atmospheric pressure fields than can be obtained in any fluid model.

A second potential advantage of digital solutions in this field is that once satisfactory numerical representations have been developed for a given class of phenomena new basins can be constructed or old ones altered by the preparation of a few punch cards. The effects of horizontal and vertical gradients of density and of the rotation of the earth can be added with much greater accuracy and less cost than in hydraulic models.

8. TESTS OF SOME DIGITAL COMPUTATIONS SCHEMES

Because digital solutions to the hydrodynamic equations have the potential ability of permitting the calculation of the effects of wind stresses and pressure gradients on the water level at the coast of an ocean or a large lake, we believe that it is necessary to exploit this technique in the study of storm surges. We also believe that the technique, when fully developed, should be very useful in engineering design studies. The development and testing of such computational models suffer from several difficulties not mentioned above. Chief among these is that surge observations obtained at the shore during storms contain an unknown increment due to the effects of surface waves. This contribution is developed in a strip less than one mile wide paralleling the coast (Dorrestein [1]; Fairchild [2]; Longuet-Higgins and Stewart [14], [15]; Saville [21]). It is not governed by equations (4)–(6) but it does appear in all of the water level observations. Next in importance are the uncertainties concerning the wind stress field. Although a solution of the equations for the wind-driven currents can provide much useful information, the computational model cannot be adequately evaluated by a direct comparison of observed and computed water levels.

A series of computational models has been developed to test the acceptability of the various finite difference expressions discussed above. The stability of each model

has been tested by introducing an applied force of the type

$$\begin{aligned} (v)\tau_h &= 0 & \text{for all } t \\ (x)\tau_h &= 0 & t \leq 0 \\ (x)\tau_h &= A [1 - \cos w t] & 0 \leq t \leq 2\pi/w \\ (x)\tau_h &= 0 & 2\pi/w \leq t \end{aligned}$$

Equilibrium conditions are assumed to prevail at $t=0$.

The total energy (kinetic+potential) of the basin is computed for each time interval. The details of this calculation are given in Appendix 1. All basins are closed with no transport across the boundaries. Each basin is rectangular in shape and is 18×18 grid steps in dimensions except where otherwise noted; since the equations are linear the absolute value of the dimensions has no bearing on the study. The pertinent facts for each model are given in the figures. As explained above, the friction term has been omitted to avoid any possible concealment of computational instability through frictional dissipation.

The first model tested was that of Fischer [3] described in Appendix 5. The energy calculations are shown in figure 2. The oscillations are due mainly to a phase difference of $(\Delta t)/2$ between the transport and height fields. The stability criterion without rotation was found to be $\Delta t < \Delta s/\sqrt{gD}/2$. The free period was approximately $26\Delta t$ units. The general features of the height and flow patterns were adequately reproduced in the model without rotation. This could be determined by comparison with an analytic solution. In the model involving rotation the inertial period from the numerical calculations was approximately $52\Delta t$ units or double the free period without rotation. The model with rotation was unstable as predicted in Fischer's theory.

The second model tested was identical to the first except that central time differences were used after the initial time step. Several methods of starting the solution were tested. The solution was not very sensitive to the starting method. The starting method adopted is described in Appendix 2. The stability criterion for the central difference form is given as $\Delta t < \Delta s/\sqrt{2gD}$, half of the value found in the previous case. The energy curves are shown in figure 3. The improvement in stability over Fischer's model is clearly evident. It was necessary to enlarge the scale in order to show evidence of variation of energy with time.

The non-rotating model reproduced the analytic solution to a high order of accuracy. No analytic solution in convenient form is known for the rotating model considered here. It was suspected that a resonance coupling between the inertial frequency and the natural frequency of the basin might be developed if the natural period were near the inertial period. In order to test this hypothesis the previous basin was adjusted to provide a natural period a little greater than $45\Delta t$ units. The resulting energy curves are shown in figure 4. The first results showed computational instability. The calculations were repeated with two smaller values of Δt without obtaining

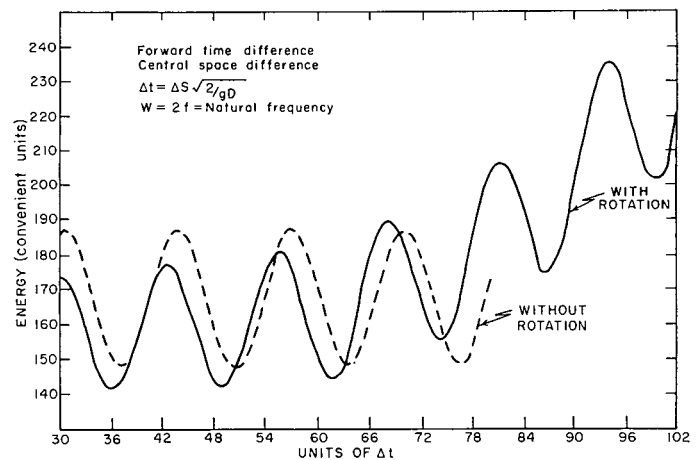


FIGURE 2.—Energy computation for Fischer's computational model, central space differences, forward or backward time differences, constant depth.

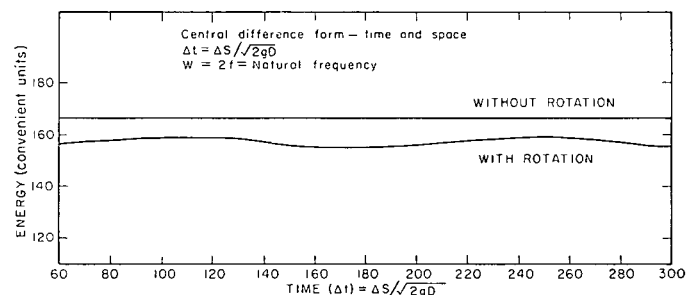


FIGURE 3.—Energy computation for model using central differences in time and space, constant depth; natural period equals one-half the inertial period for rotating model.

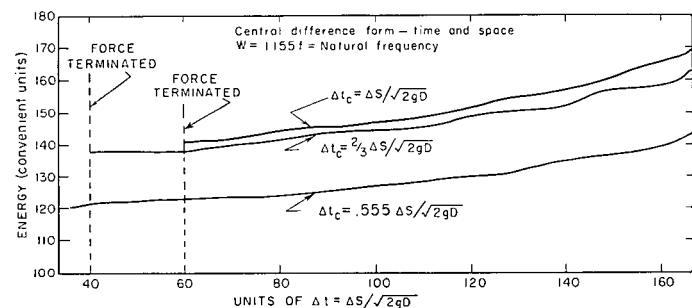


FIGURE 4.—Same as figure 3, except that the natural period equals 0.864 of the inertial period.

any substantial improvement. It appears from these tests that the central difference formulation of the problem is nearly stable if the frequency of the motion is very different from the inertial period, but quickly becomes unstable if the natural and inertial periods are similar. In the general storm surge problem, however, one cannot be sure that the natural period or the forcing period will not

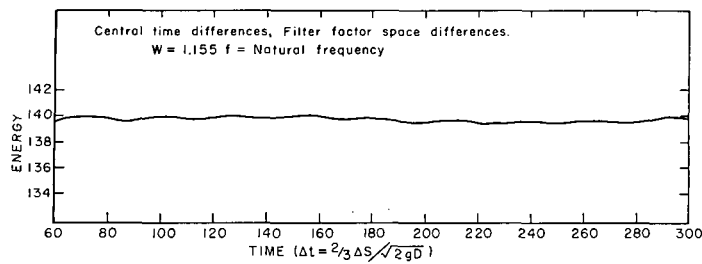


FIGURE 5.—Same as figure 4, except that the filter factor form is used for space differences.

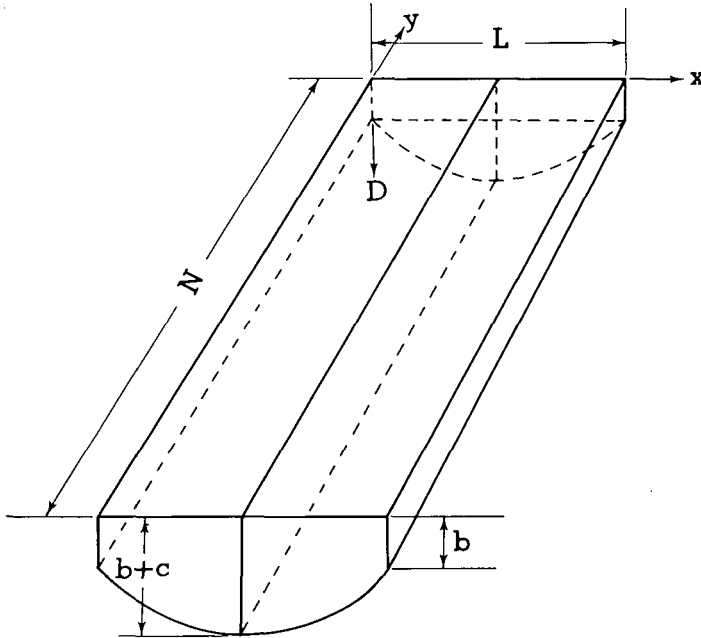


FIGURE 6.—Schematic illustration of the variable depth basin used in testing computational stability.

approach the inertial period, therefore the search for a more stable computational system was continued.

The third model tested was identical to the last in its physical characteristics. However, the filter factor form was used. Several subtle changes in the numerical analysis are required to obtain a consistent set of prediction equations. In order not to interrupt the present flow of thought on the computational stability problem, a detailed discussion of these changes is deferred to Appendix 4. The important consideration here is the improvement in computational instability obtained with the filter factor form, as shown by the energy curve in figure 5. Again it became necessary to expand the scale to show any variation of energy. This form appears to be sufficiently stable, even when Coriolis terms are included.

In the fourth test, the constant depth was replaced by the depth law

$$D(x, y) = -\frac{4C}{L^2} x^2 + \frac{4C}{L} x + b \quad (28)$$

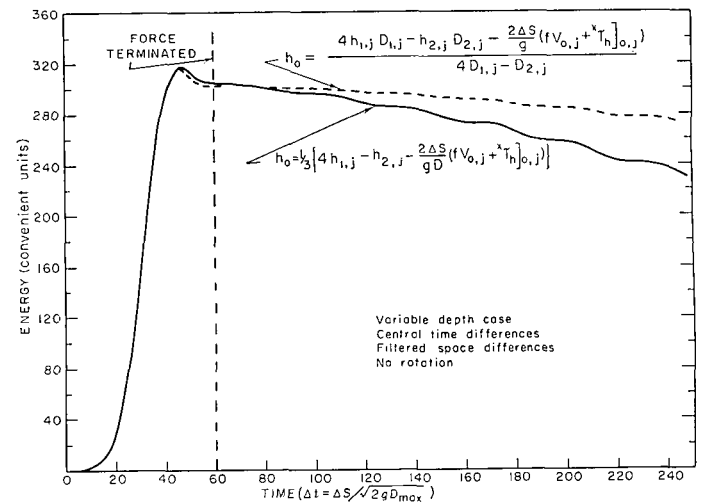


FIGURE 7.—Energy calculation for variable depth model with stress parallel to the depth contours, central time differences, filtered factor space differences, no rotation.

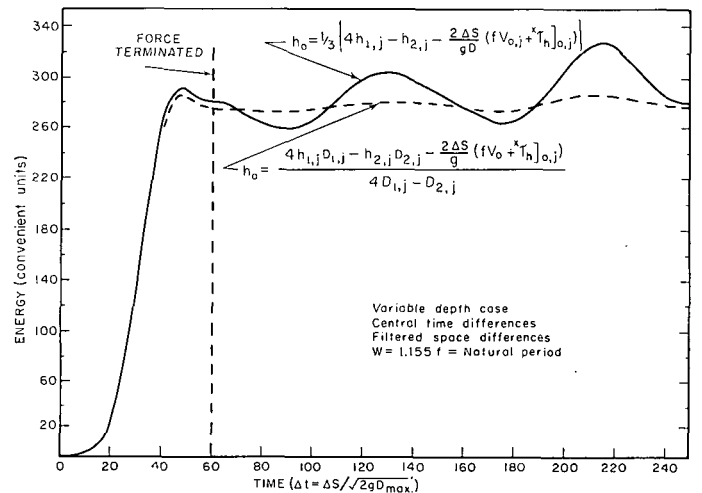


FIGURE 8.—Same as figure 7, but with rotation.

depicted in figure 6. No instabilities were observed with or without rotation of the basin on a $36 \times 36 \Delta s$ grid. The results are not shown.

The fifth test was identical with the preceding one, except that the depth law was changed to

$$D(x, y) = -\frac{4C}{L^2} y^2 + \frac{4C}{L} y + b.$$

This is equivalent to rotating the basin shown in figure 6 by 90° so that the stress is parallel to the bottom contours.

The energy curves obtained from an $18 \times 18 \Delta s$ grid without rotation are shown in figure 7. The solid curve was obtained with boundary conditions of the form of equation (25). The dashed line was obtained with boundary conditions of the form of equation (27). Here it is

seen that the form of the boundary conditions can affect the computational stability and that instability may take the form of a gradual loss as well as a growth of energy.

The energy curves obtained with rotation are shown in figure 8. The solid line was obtained with equation (25) and the dashed line with (27). The flow patterns of the variable depth models are more complex than those of the constant depth models. Thus a better description of the flow and an improvement in the computational stability can be obtained by using smaller values of Δx . This is particularly true when the rotation of the earth is considered.

9. THE PHYSICS OF THE DISSIPATION PROCESS

The least understood of the problems involved in the construction of hydraulic models is the proper method of dissipating energy. A physical analysis of the problem indicates that the principal cause of dissipation over a rigid bottom in shallow water is skin friction and that this should depend on the bottom roughness and the velocity vector near the bottom. The resulting stress is proportional to the velocity gradient at the bottom and is believed to be proportional to the square of the speed at the upper limit of the boundary layer, and directed oppositely to the bottom current vector. However, the calculations discussed above provide values only for the mean current averaged throughout the depth of the fluid. In severe storms, the instantaneous motion at the bottom may be dominated by wind waves and swell to a depth of a hundred feet, and even the resultant motion, averaged over many wave periods, may have any orientation relative to the mean current motion. The direction, as well as the magnitude, of the bottom stress vector is frequently indeterminable from the other information provided by the calculation.

The above considerations apply to both physical and mathematical models. When only the transient periods involving the build-up of a disturbance are considered, the quantitative accuracy of published computations appears to be independent of the assumptions made about the bottom stress, and a wide range of assumptions has been used. This suggests that equally good results might be obtained for the transient case by neglecting the dissipation term altogether. This procedure cannot be used in studying the decay of an unusual disturbance or in studying quasi-steady state solutions which require the operation of the model for several prototype days or weeks. In these cases some dissipative mechanism must be included to obtain a reasonable balance of energy. Any scheme which achieves a reasonable balance of energy can be expected to provide a reasonable picture of the main features of the flow, but only the scheme which is locally correct will give a good reproduction of small-scale features.

The use of hydraulic models avoids the necessity of a clear statement of the law governing the dissipation of energy. This does not mean that it avoids the errors

resulting from using an unsatisfactory law. If the model is calibrated for calm weather conditions it can be expected to underestimate the friction effects during storms. If calibrated for storm conditions it can be expected to overestimate friction during calm weather conditions.

10. THE COMPUTATION OF DISSIPATION TERMS

Although the proper expression for the physical dissipation term has not been uniquely determined, it is safe to say that its effect should be to decrease the total energy of the flow. However, the straightforward introduction of the dissipation term into central difference formulas usually leads to computational instability, that is, to an increase in the energy of the computed flow. This may be avoided by evaluating the velocity at time $t - \Delta t$ when computing the dissipation term in a model in which central differences are used for all other terms, or an implicit method may be used. A more detailed discussion of this computational problem has been given by Miyakoda [16] and Platzman [18].

11. SUMMARY AND FUTURE OUTLOOK

It has been shown that the computational stability and hence the reliability of numerical solutions of the hydrodynamic equations may depend on the particular manner in which the terms and differential quotients of the differential equations and the boundary conditions are approximated by finite difference expressions. It has been pointed out, but not explicitly demonstrated, that the errors resulting from an unsatisfactory method of approximations to the terms and differential quotients generally take the form of false disturbances with horizontal scales of only a few mesh lengths in both the velocity and height fields. Small-scale disturbances in the grid system can be eliminated or at least suppressed by the use of appropriate filter functions. However, the filtering operators will affect both the true small-scale disturbance which is a part of the physical problem and the false small-scale disturbance which results from the numerical process in the same manner. Thus it is not possible to obtain a true solution when the numerical process applied generates disturbances of the same scale as the real disturbances.

This difficulty, which is of a mathematical nature, can be avoided by using mesh lengths much smaller than the scale of any important phenomenon to be investigated. This result could be obtained in a straightforward manner by using uniformly spaced computation points over the entire basin, and magnetic tapes or other devices for increasing the storage capacity of a computer. This is rather expensive because the permissible value of Δt is limited proportionally to $\Delta x / \sqrt{gD}$. Space detail is generally needed only in shallow water, but the existence of deep water constrains one to compute excessive time detail as well. The same result can be obtained by using a smaller mesh length in regions where small-scale phenomena are important, and a greater mesh length in other

regions. Experiments now being conducted by the authors and their associates indicate that this process will produce satisfactory results but that this problem is no more simple than the construction of an optimum finite difference form.

Although no data on the solution of practical problems are contained in this paper, references have been made to several studies by Hansen, Platzman, Welander, and others in which excellent agreement was obtained between numerical solutions of the equations and the large-scale features of geophysical phenomena. In most cases the computations also show small-scale phenomena of greater intensity than that observed in nature, and not very well correlated with the observed small-scale phenomena.

The problem of energy dissipation is of a more fundamental nature. One other problem of a similar nature is also important. This is the specification of the wind stress field. In both of these cases the difficulty is due to the lack of a satisfactory physical model relating the transfer of momentum by turbulence to the time-averaged flow of a fluid. In the first approximation the difficulty amounts to an imprecise knowledge of a momentum transfer coefficient such as the drag coefficient for wind over water, or water over the bottom of the basin. In both cases some improvement in the numerical solution can be obtained by calibrating it to past observations by experimenting with the transfer coefficients, in much the same way as one calibrates a hydraulic model by varying the roughness parameter. The process is not very satisfying from a scientific point of view, but it can be used to obtain useful results.

The authors must decry a prevailing tendency in this field to try to match a poorly understood dissipation mechanism to a poorly understood computational instability problem in the hope that the two errors will cancel each other.

The nature of the computational difficulties is well enough understood to enable one to obtain considerable insight into the nature of many problems even though quantitatively exact answers may not be available. For example, numerical computations may be used to determine the relative severity of the surge expected to accompany an arbitrary storm approaching the coast from several directions. This concept has been used as the basis of a successful system for predicting the seiches occasionally produced in Chicago by squall lines. Numerical calculations by present methods can be expected to reveal the response of a harbor as a whole to any large-scale disturbance outside the harbor, but the hydrodynamic calculations discussed here cannot yet be depended on to reveal information on the effects of breakwaters or wave run-up, or intersecting wave trains. Other types of calculations, such as wave refraction diagrams based on geometrical optics, may be useful in solving such problems.

APPENDIX 1.—ENERGY CALCULATIONS

The energy invariant for equations (4), (5), (6) without the friction and forcing terms is

$$E = \frac{\rho}{2} \int_A \left(gh^2 + \frac{U^2 + V^2}{D} \right) dA$$

where A is the surface area of the basin. Since the transports and height values are known only at discrete points of a grid system, the energy equation can be solved only by recourse to a numerical quadrature. Throughout this paper, the three fields are calculated at each and every grid point, including the boundaries, for each time interval.

Consider a rectangular (LW) grid whose points on L run from 0 to L , and on W run from 0 to W . By noting that the boundary conditions oblige the transports normal to the boundaries and at the corners to be zero, energy for the rectangular basin at a given time can be approximated by the trapezoidal rule to

$$\begin{aligned} E^* = \frac{2E}{\rho(\Delta s)^2} \approx & \sum_{i=1}^{L-1} \sum_{j=1}^{W-1} [g(h_{i,j})^2 + \{ (U_{i,j})^2 + (V_{i,j})^2 \} / D_{i,j}] \\ & + \frac{1}{2} \sum_{j=1}^{W-1} [g\{ (h_{0,j})^2 + (h_{L,j})^2 \} + \{ (U_{0,j})^2 + (V_{0,j})^2 \} / D_{0,j} \\ & + \{ (U_{L,j})^2 + (V_{L,j})^2 \} / D_{L,j}] + \frac{1}{2} \sum_{i=1}^{L-1} [g\{ (h_{i,0})^2 \\ & + (h_{i,W})^2 \} + \{ (U_{i,0})^2 + (V_{i,0})^2 \} / D_{i,0} + \{ (U_{i,W})^2 \\ & + (V_{i,W})^2 \} / D_{i,W}] + \frac{g}{4} [(h_{0,0})^2 + (h_{0,W})^2 + (h_{L,0})^2 + (h_{L,W})^2] \end{aligned}$$

where $h_{i,j} = h(i\Delta s, j\Delta s, t)$, $u_{i,j} = u(i\Delta s, j\Delta s, t)$, $v_{i,j} = v(i\Delta s, j\Delta s, t)$. The quantity E^* is the energy term calculated here in machine computations for convenience.

APPENDIX 2.—STARTING PROCEDURE

If central differences are used and calculations are for each grid point at each time period, it is necessary to know the field values of U , V , and h at time t and $t-1$ in order to calculate the values at time $t+1$. Thus some alternative procedure must be used for calculations at time $t=1$. This requirement is avoided when only forward differences are used in time, or when the staggered grid system is employed; however, there are other disadvantages to these systems. Since all grid points are used at each time step in this study, special starting procedures are required utilizing a forward difference scheme for the first time interval.

Since the field values are zero initially and the forcing function is small at the first time interval, the momentum equations of motion are approximated at interior points to,

$$\frac{\partial U}{\partial t} \approx fV + {}^{(x)}\tau$$

$$\frac{\partial V}{\partial t} \approx -fU + {}^{(y)}\tau$$

Applying a forward difference to the time derivatives above and taking the arithmetic mean in time for the right-hand side of the equations give,

$$U_{i,j} \approx \frac{\Delta t}{2} [{}^{(x)}\tau_{i,j} + fV_{i,j}]$$

$$V_{i,j} \approx \frac{\Delta t}{2} [{}^{(y)}\tau_{i,j} - fU_{i,j}]$$

When the principal part of each transport term is chosen for the Coriolis cross term, the above is further approximated to

$$U_{i,j} \approx \frac{\Delta t}{2} \left[{}^{(x)}\tau_{i,j} + \frac{f\Delta t}{2} {}^{(y)}\tau_{i,j} \right]$$

$$V_{i,j} \approx \frac{\Delta t}{2} \left[{}^{(y)}\tau_{i,j} - \frac{f\Delta t}{2} {}^{(x)}\tau_{i,j} \right]$$

The starting values for the transport terms are now substituted in the equation of continuity, with similar reasoning as above, to give height values at the interior points as

$$h_{i,j} \approx \frac{\Delta t}{4\Delta s} [U_{i+1,j} - U_{i-1,j} + V_{i,j+1} - V_{i,j-1}]$$

Note that $h_{i,j}$ is zero everywhere in the interior for the type force used in this study except for points on the first mesh lines bordering the boundaries.

A starting procedure for the boundaries can now be formulated. Consider the west wall where the U transport is zero for all time. In this case the V transport is,

$$V_{0,j} \approx \frac{\Delta t}{2} {}^{(y)}\tau_{0,j}$$

For the force considered in this paper, $V_{0,j}^1$ is zero. Similar considerations hold for the other boundaries. The boundary conditions of equation (25) utilizing a forward differencing in space give

$$h_{0,j}^1 = h_{1,j}^1 - \frac{\Delta s}{gD_{0,j}} [fV_{0,j}^1 + {}^{(x)}\tau_{0,j}^1]$$

Similar forms are developed for the other boundaries.

For the corner points, a method is given in Appendix 3.

Tests made with several different types of starting procedures gave results which appear to show that the numerical solution for a rectangular basin, initially quiescent, is not sensitive to the starting procedure used for the type force considered in this study.

For some numerical runs with different starting procedures, the height values of the boundary points after each interval of machine calculations were stored on magnetic tape for future use. The same problem was then rerun with the stored height values as boundary conditions to see if zero normal transport could be recaptured on the boundaries. For these tests, the starting procedure was superior to others tried and did recapture zero normal transports at the boundaries except for minor errors on the corner points.

APPENDIX 3.—CORNER POINTS

The corner points of a rectangular grid have zero transports; therefore $\partial U/\partial t$, $\partial V/\partial t$ are also zero. This suggests using both momentum equations weighted equally to determine height values at the corners. Consider the SW corner at point (0,0). The two momentum equations give

$$\frac{\partial h}{\partial x} = \frac{{}^{(x)}\tau}{gD}, \quad \frac{\partial h}{\partial y} = \frac{{}^{(y)}\tau}{gD}$$

Expanding the above derivatives as in (13), adding and arranging gives,

$$h_{0,0}^m = \left[4(h_{0,1}^m + h_{1,0}^m) - h_{0,2}^m - h_{2,0}^m - \frac{2\Delta s}{gD_{0,0}} ({}^{(x)}\tau_{0,0}^m + {}^{(y)}\tau_{0,0}^m) \right] / 6$$

For starting values, a simple forward difference of the two momentum equations gives

$$h_{0,0}^1 = \left[h_{0,1}^1 + h_{1,0}^1 - \frac{\Delta s}{gD_{0,0}} ({}^{(x)}\tau_{0,0}^1 + {}^{(y)}\tau_{0,0}^1) \right] / 2$$

The momentum equations can also be combined to give a slightly different compact form.*

$$h_{0,0}^m = \left\{ \begin{vmatrix} -1 & 0 & -1 \\ 4 & 4 & 0 \\ 0 & 4 & -1 \end{vmatrix} h_{1,1}^m - \frac{4\Delta s}{gD_{0,0}} [{}^{(x)}\tau_{0,0}^m + {}^{(y)}\tau_{0,0}^m] \right\} / 9$$

Application of (27) to the two momentum equations gives, for variable depths,

$$h_{0,0}^m = \frac{\begin{vmatrix} -1 & 0 & -1 \\ 4 & 4 & 0 \\ 0 & 4 & -1 \end{vmatrix} (Dh)_{1,1}^m - \frac{4\Delta s}{g} [{}^{(x)}\tau_{0,0}^m + {}^{(y)}\tau_{0,0}^m]}{\begin{vmatrix} -1 & 0 & -1 \\ 4 & 4 & 0 \\ 0 & 4 & -1 \end{vmatrix} D_{1,1}}$$

Similar results hold for the other three corner points. Notice that the height values at the corner points are determined last, after field values are determined at the interior and boundary points.

APPENDIX 4.—SMOOTHING THE CENTRAL DIFFERENCE FORM

The growth of energy in the runs of the central difference form may be attributed to the interaction of high frequency components for which the grid system is incapable of discriminating correctly. The smallest wavelength for which the grid system is capable of discriminating is $2\Delta s$; this wavelength is the one most likely to arise from truncation error and therefore the one most likely to

*The form can be derived from a Taylor expansion in two dimensions or applications of (13).

degrade the solution with time. By use of a smoothing routine, wavelength components of $2\Delta s$ may be suppressed from the field at given times (Shuman [22]). An elementary smoothing function in one-dimension acting on a field F at discrete interior points (i, j) of a grid system can be,

$$\tilde{F}_{i,j} = \frac{1}{4} [F_{i-1,j} + 2F_{i,j} + F_{i+1,j}] = \frac{1}{4} \begin{vmatrix} 1 & 2 & 1 \end{vmatrix} F_{i,j}$$

In two dimensions, one could smooth first in one direction and then smooth the smoothed value in the other to obtain,

$$\tilde{\tilde{F}} = \frac{1}{4} \begin{vmatrix} \tilde{F}_{i,j+1} \\ 2\tilde{F}_{i,j} \\ \tilde{F}_{i,j-1} \end{vmatrix} = \frac{1}{16} \begin{vmatrix} 1 & 2 & 1 \\ 2 & 4 & 2 \\ 1 & 2 & 1 \end{vmatrix} F_{i,j}$$

It is irrelevant in which direction smoothing is first applied. The 9-point form can be applied to the field values of interior points while the 3-point form can be applied to the boundaries. No known symmetric smoothing form can be applied to the corner points.

It is possible to keep the program loops which compute the field quantities for time $t+1$ distinct from the smoothing loops, and in fact this procedure is frequently followed. Some advantages can be gained by combining the two processes. If the 9-point smoothing form is applied to the derivatives of the central difference form, say, in the x -direction, there follows,

$$\begin{aligned} \left(\frac{\partial F}{\partial x} \right)_{F=F_{i,j}} &= \frac{1}{2\Delta s} [-\tilde{\tilde{F}}_{i-1,j} + \tilde{\tilde{F}}_{i+1,j}] \\ &= \frac{1}{32\Delta s} \begin{vmatrix} -1 & -2 & 0 & 2 & 1 \\ -2 & -4 & 0 & 4 & 2 \\ -1 & -2 & 0 & 2 & 1 \end{vmatrix} F_{i,j} \end{aligned}$$

If the following approximation is considered,

$$\frac{1}{32\Delta s} \begin{vmatrix} -1 & 0 & 0 & 0 & 1 \\ -2 & 0 & 0 & 0 & 2 \\ -1 & 0 & 0 & 0 & 1 \end{vmatrix} F_{i,j} \approx \frac{1}{16\Delta s} \begin{vmatrix} -1 & 0 & 1 \\ -2 & 0 & 2 \\ -1 & 0 & 1 \end{vmatrix} F_{i,j}$$

then the derivative can be rewritten as,*

$$\left(\frac{\partial F}{\partial x} \right)_{F=F_{i,j}} = \frac{1}{8\Delta s} \begin{vmatrix} -1 & 0 & 1 \\ -2 & 0 & 2 \\ -1 & 0 & 1 \end{vmatrix} F_{i,j}$$

and

$$\left(\frac{\partial F}{\partial y} \right)_{F=F_{i,j}} = \frac{1}{8\Delta s} \begin{vmatrix} 1 & 2 & 1 \\ 0 & 0 & 0 \\ -1 & -2 & -1 \end{vmatrix} F_{i,j}$$

These expressions are of the same form as equation (15). This derivation explains the name "filter factor form" (Shuman [23]) and the choice of the constants a and b .

This derivation also shows that all finite difference operators have some characteristics of smoothing operators. It appears that terms which are not differenced should be smoothed by a similar smoothing function. Experiments not discussed in this report indicate that this procedure improves the stability of the calculations. The filter factor forms of the equations of motion, as used in this study, are given below. Note that the Coriolis terms are smoothed.

If the area 9-point smoothing form and the above altered derivative forms are applied to the field values at time m in the equations of motion for the central difference form, the following results:

$$\begin{aligned} U_{i,j}^{m+1} &= U_{i,j}^{m-1} - gD_{i,j} \frac{\Delta t}{4\Delta s} \begin{vmatrix} -1 & 0 & 1 \\ -2 & 0 & 2 \\ -1 & 0 & 1 \end{vmatrix} h_{i,j}^m \\ &\quad + \frac{f\Delta t}{8} \begin{vmatrix} 1 & 2 & 1 \\ 2 & 4 & 2 \\ 1 & 2 & 1 \end{vmatrix} V_{i,j}^m + 2\Delta t^{(x)} \tau_{i,j}^m \\ V_{i,j}^{m+1} &= V_{i,j}^{m-1} - gD_{i,j} \frac{\Delta t}{4\Delta s} \begin{vmatrix} 1 & 2 & 1 \\ 0 & 0 & 0 \\ -1 & -2 & -1 \end{vmatrix} h_{i,j}^m \\ &\quad - \frac{f\Delta t}{8} \begin{vmatrix} 1 & 2 & 1 \\ 2 & 4 & 2 \\ 1 & 2 & 1 \end{vmatrix} U_{i,j}^m + 2\Delta t^{(y)} \tau_{i,j}^m \\ h_{i,j}^{m+1} &= h_{i,j}^{m-1} - \frac{\Delta t}{4\Delta s} \left\{ \begin{vmatrix} -1 & 0 & 1 \\ -2 & 0 & 2 \\ -1 & 0 & 1 \end{vmatrix} U_{i,j}^m \right. \\ &\quad \left. + \begin{vmatrix} 1 & 2 & 1 \\ 0 & 0 & 0 \\ -1 & -2 & -1 \end{vmatrix} V_{i,j}^m \right\} \end{aligned}$$

Note that in boundary computations using the one-dimensional smoothing operator, the Coriolis cross term is absent and the derivative remains unchanged from a similar approximation as in the two-dimensional form. The central difference form thus can be applied directly to the boundaries without any alterations.

Some further characteristics of the filter factor form of the equations can be illustrated by considering the free

*If $F(x, y)$ is expanded in a Taylor series up to and including the 2d derivatives about eight neighboring points, one can form,

$$\frac{\partial F}{\partial x} = \frac{1}{2(b+2a)\Delta s} \begin{vmatrix} -a & 0 & a \\ -b & 0 & b \\ -a & 0 & a \end{vmatrix} F_{i,j}$$

where a and b are parameters at disposal. In the central difference form a is taken as zero. In this study, a is 1 and b is 2.

oscillations of a constant depth basin in the absence of the Coriolis and force terms. Let the solution for the transport and height fields have formal solutions of individual terms,

$$(U, V, h)^{m\Delta t} = (U, V, h)^0 \lambda^m$$

where $(U, V, h)^0 \propto e^{\sqrt{-1}\Delta s(a+ib)}$ and $a=2\pi/L$, $b=2\pi/W$ are spatial wave numbers. The formal solution permits,

$$(U, V, h)^{(m+1)\Delta t} = \lambda^2 (U, V, h)^{(m-1)\Delta t}$$

$$(U, V, h)^{m\Delta t} = \lambda (U, V, h)^{(m-1)\Delta t}$$

The filter factor form may now be written as,

$$\begin{bmatrix} \lambda^2 - 1 & 0 & \sqrt{-1}\alpha\nu'\lambda \\ 0 & \lambda^2 - 1 & \sqrt{-1}\alpha\nu''\lambda \\ \sqrt{-1}\beta\nu'\lambda & \sqrt{-1}\beta\nu''\lambda & \lambda^2 - 1 \end{bmatrix} \begin{bmatrix} U^{m-1} \\ V^{m-1} \\ h^{m-1} \end{bmatrix} = 0$$

where, $\alpha = \frac{gD\Delta t}{4\Delta s}$, $\beta = \frac{\Delta t}{4\Delta s}$, $\nu' = 4 \sin a\Delta s(1 + \cos b\Delta s)$, and $\nu'' = 4 \sin b\Delta s(1 + \cos a\Delta s)$

Suppose now that L or W has wavelength $2\Delta s$. The terms ν' , and ν'' in the matrix disappear so that wavelengths of $2\Delta s$ are deleted from the computations.*

In order for the matrix form to hold,

$$(\lambda^2 - 1)[(\lambda^2 - 1)^2 + \alpha\beta(\nu'^2 + \nu''^2)\lambda^2] = 0$$

or

$$\lambda^4 + 2 \left[\frac{\alpha\beta(\nu'^2 + \nu''^2)}{2} - 1 \right] \lambda^2 + 1 = 0$$

For stability, it is required (Richtmyer [20]) that $|\lambda| \leq 1$. For this to hold, the above equation gives,

$$\frac{\alpha\beta(\nu'^2 + \nu''^2)}{4} < 1$$

Noting that the max of ν' and ν'' is 8, then substitution in the above equation gives a stability criterion of,

$$\Delta t < \frac{\Delta s}{\sqrt{2gD}}$$

This criterion is identical to that of the central difference form.

APPENDIX 5.—FISCHER'S FORM

The finite difference form given by Fischer [3] uses forward differences in time and central differences in space. It is a combination of explicit and implicit methods. For interior points, neglecting bottom stress and incorporating the pressure force term with τ the surface stress term, the form is,

$$U_{i,j}^{m+1} = U_{i,j}^m - \frac{g\Delta t}{2\Delta s} D_{i,j}[h_{i+1,j}^m - h_{i-1,j}^m] + \Delta t[fV_{i,j}^m + {}^{(z)}\tau_{i,j}^m]$$

$$V_{i,j}^{m+1} = V_{i,j}^m - \frac{g\Delta t}{2\Delta s} D_{i,j}[h_{i,j+1}^m - h_{i,j-1}^m] - \Delta t[fU_{i,j}^m - {}^{(w)}\tau_{i,j}^m]$$

$$h_{i,j}^{m+1} = h_{i,j}^m - \frac{\Delta t}{2\Delta s} [U_{i+1,j}^{m+1} - U_{i-1,j}^{m+1} + V_{i,j+1}^{m+1} - V_{i,j-1}^{m+1}]$$

where the notation follows that of equations (1)–(3). It can be shown that for constant depth, no Coriolis, and free oscillations, a stability criterion for the simple wave equation is,

$$\Delta t < \sqrt{\frac{2}{gD}} \Delta s$$

Fischer's form is appealing since field values for time $(m-1)\Delta t$ are not required in the calculations, the stability criterion is twice that of the central difference form, and starting values are not needed. For the case of rotation with constant depths and a periodic boundary condition that permits a solution in a Fourier expansion, the form is unstable unless the bottom stress term in the difference form is retained as a frictional dissipation term. The friction term as given by Fischer is, ${}^{(z)}\tau_{-D} = rU$; ${}^{(w)}\tau_{-D} = rV$, where r is a coefficient generally given as a function that varies inversely as some power of the depth. For this case, Fischer shows that the difference form is stable provided that

$$\Delta t < r/f^2; \quad f \neq 0$$

REFERENCES

1. R. Dorrestein, "Wave Set-Up on a Beach," pp. 230–241 of "Proceedings of the Second Technical Conference on Hurricanes," *National Hurricane Research Project Report No. 50*, U.S. Weather Bureau, 1962.
2. J. Fairchild, "Model Study of Wave Set-Up Induced by Hurricane Waves at Narragansett Pier, Rhode Island," *Bulletin of the Beach Erosion Board*, vol. 12, 1958, pp. 9–20.
3. G. Fischer, "Ein numerisches Verfahren zur Errechnung von Windstau und Gezeiten in Randmeeren," *Tellus*, vol. 11, No. 1, Feb. 1959, pp. 60–76.
4. H. Fortak, "Concerning the General Vertically Averaged Hydrodynamic Equations with Respect to Basic Storm Surge Equations," *National Hurricane Research Project Report No. 51*, U.S. Weather Bureau, 70 pp. 1962.
5. W. Hansen, "Theorie zur Errechnung des Wasserstandes und der Strömungen in Randmeeren nebst Anwendungen," *Tellus*, vol. 18, No. 3, Aug. 1956, pp. 287–300.
6. W. Hansen, "Hydrodynamical Methods Applied to Oceanographic Problems," *Proceedings of the Symposium on Mathematical-Hydrodynamical Methods of Physical Oceanography*, Institut für Meereskunde der Universität Hamburg, 1962, pp. 25–34.
7. D. L. Harris, "The Equivalence between Certain Statistical Prediction Methods and Linearized Dynamical Methods," *Monthly Weather Review*, vol. 90, No. 8, Aug. 1962, pp. 331–340.
8. D. L. Harris, "Characteristics of the Hurricane Storm Surge," *Technical Paper No. 48*, U.S. Weather Bureau, 1963, 139 pp. (see pp. 6–7).

*In the central difference form, wavelengths of $2\Delta s$ do not conveniently drop out since ν' and ν'' do not have the multiplication term, $(1 + \cos^2 \Delta s)$.

9. D. L. Harris and A. Angelo, "A Regression Model for Storm Surge Prediction," *Monthly Weather Review*, vol. 91, nos. 10-12, Oct.-Dec. 1963, pp. 710-726.
10. D. L. Harris, N. A. Pore, and R. Cummings, "The Application of High Speed Computers to Practical Tidal Problems," 1963. (unpublished.)
11. B. Haurwitz, "The Slope of Lake Surfaces under Variable Wind Stresses," *Technical Memorandum* No. 25, Beach Erosion Board, 1951.
12. J. Holloway, "Smoothing and Filtering of Time Series and Space Fields," *Advances in Geophysics*, vol. 4, 1958, pp. 351-389.
13. H. Lauwerier, "Some Recent Work of the Amsterdam Mathematical Center on the Hydrodynamics of the North Sea," *Proceedings of the Symposium on Mathematical-Hydrological Methods of Physical Oceanography*, Institut für Meereskunde der Universität Hamburg, 1962, pp. 13-24.
14. M. S. Longuet-Higgins and R. W. Stewart, "A Note on Wave Set-Up," *Journal of Marine Research*, vol. 21, No. 1, Jan. 1963, pp. 4-10.
15. M. S. Longuet-Higgins and R. Stewart, "Radiation Stress and Mass Transport in Gravity Waves with Application to 'Surf Beats,'" *Journal of Fluid Mechanics*, vol. 13, No. 4, Aug. 1962, pp. 481-504.
16. K. Miyakoda, "Contribution to the Numerical Weather Prediction: Computation with Finite Difference," *Japanese Journal of Geophysics*, vol. 3, No. 1, Mar. 1962, pp. 75-190.
17. G. Platzman, "The Lattice Structure of the Finite-Difference Primitive and Vorticity Equations," *Monthly Weather Review*, vol. 86, No. 8, Aug. 1958, pp. 285-292.
18. G. Platzman, "The Dynamical Prediction of Wind Tide on Lake Erie," *Technical Report* No. 7, Contract Cwb-9768, Department of Geophysical Sciences, University of Chicago, 1963.
19. N. A. Pore, "The Relation of Wind and Pressure to Extratropical Storm Surges at Atlantic City," *Journal of Applied Meteorology*, vol. 3, No. 2, Apr. 1964, pp. 155-163.
20. R. Richtmyer, "Difference Methods for Initial Value Problems," *Interscience*, No. 4, 1957.
21. T. Saville, Jr., "Experimental Determination of Wave Set-up," pp. 242-252 in "Proceedings of the Second Technical Conference on Hurricanes," *National Hurricane Research Project Report* No. 50, U.S. Weather Bureau, 1962.
22. F. Shuman, "Numerical Methods in Weather Prediction: II. Smoothing and Filtering," *Monthly Weather Review*, vol. 85, No. 11, Nov. 1957, pp. 357-361.
23. F. Shuman, "Numerical Experiments with the Primitive Equations," *Proceedings of the International Symposium on Numerical Weather Prediction*, Tokyo, Nov. 7-12, 1960, Meteorological Society of Japan, 1962, pp. 85-108.
24. P. Welander, "Numerical Prediction of Storm Surges," *Advances in Geophysics*, vol. 8, 1961, pp. 316-379.

[Received November 10, 1963; revised February 13, 1964]